

Chaos and two-level dynamics of the Atomtronic Quantum Interference Device

Geva Arwas, Doron Cohen

Department of Physics, Ben-Gurion University, Beer-Sheva 84105, Israel

Abstract. We study the Atomtronic Quantum Interference Device employing a semiclassical perspective. We consider an M site ring that is described by the Bose-Hubbard Hamiltonian. Coherent Rabi oscillations in the flow of the current are feasible, with an enhanced frequency due to chaos-assisted tunneling. We highlight the consequences of introducing a weak-link into the circuit. In the latter context we clarify the phase-space considerations that are involved in setting up an effective “systems plus bath” description in terms of Josephson-Caldeira-Leggett Hamiltonian.

1. Introduction

Atomtronic is a new quantum technology [1, 2], with potential for novel quantum computing implementations [3, 4, 5, 6]. Theory and experiments with Atomtronic superfluid circuits are in the focus of current research [7, 8, 9, 10]. A major objective is to realize a Quantum Interference Device (AQUID) that possibly includes one or two weak-links [11]. This is analogous to a superconducting circuit, or to its low dimensional version (fluxon, Josephson vortex qubit) [12, 13, 14, 15]. However the design considerations of such device are still somewhat vague.

We study an Atomtronic superfluid circuit that is described by the Bose-Hubbard Hamiltonian (BHH) [5]. Namely, we consider N bosons in an M site rotating ring such that the model parameters are (N, M, K, U, Φ) , where K is the hopping frequency between the sites, U is the on-site interaction, and the rotation is formally equivalent to having an Aharonov-Bohm flux Φ . If a weak-link is introduced, there is an additional parameter α that characterizes the relative strength of the coupling.

For the purpose of qubit realization, the objective is to single out a two-level system (TLS) that is quasi-isolated from all the other microscopic degrees of freedom (DOFs). In the present context there are two flow-states that differ by their “winding number” m , meaning that they are characterized by a different value of the persistent current (I_m). The flow-states are required to be meta-stable, meaning that each of them will not decay in time. If they are quasi-degenerate, one would like to witness coherent Rabi oscillations. During a Rabi-based protocol the system evolves into a superposition of macroscopically distinct flow-states [16].

The introduction of a weak-link allows control over the coupling Δ_s between the flow-states. Without a weak-link this coupling might be too small for operational purpose, meaning that the time period ($2\pi/\Delta_s$) of coherent Rabi oscillations might become too large for practical implementations. On the other hand if the relative strength of the weak-link (α) is smaller than some critical value, then the meta-stability is destroyed, which is effectively like having a disconnected ring. The dependence of Δ_s on N and on M in the case of an AQUID has been recently addressed in Ref.[6] following [10], highlighting the subtle interplay of interactions and quantum fluctuations. The present work is in a sense complementary and provides a semi-classical perspective for the analysis of a few-site ring that is described by the BHH, with or without a weak-link.

Formally our BHH system has $d = M-1$ coupled DOFs: the dimer ($M = 2$) is the so-called bosonic Josephson junction; while the trimer ($M = 3$) is the minimal superfluid circuit. Our main focus is on BHH circuits with small number of sites. The following specific questions arise: **(A)** In what range of the model parameters is it possible to have metastable flow-states? **(B)** Can we treat two quasi-degenerate flow-states as a coherent two-level-system? If yes, **(C)** how the frequency of the coherent Rabi oscillation is determined? And if a weak-link is introduced then, **(D)** can we derive the dynamics from an effective “system plus bath” Hamiltonian. Question (A) has been partially addressed in our previous publications [17, 18], and its physics is briefly summarized in Appendix A. In the present work we would like to further address questions (B-D).

Our main observations are: **(1)** In the absence of a weak-link, coherent Rabi oscillations are feasible, with frequency that is possibly determined by chaos-assistance tunneling, leading to weaker dependence on the number of particles. **(2)** In particular we demonstrate numerically Rabi oscillations between metastable flow-states in a non-rotating ($\Phi = 0$) circuit that consists of $M = 4$ sites. **(3)** We find what is the critical strength of a weak-link, below which superfluidity is diminished. **(4)** We illuminate how our considerations connect with the familiar “system plus bath” framework of Caldeira and Leggett. **(5)** We show that with weak-link the threshold to chaos is pushed up in energy, which is a necessary condition for the validity of the single Josephson-junction description. **(6)** We point out that the requirement for observing coherent Rabi oscillation in large M rings might be in clash with the quantum Mott transition.

The outline is as follows: In Section 2 we introduce the model and the methods; In Section 3 we discuss the coherent dynamics in the absence of a weak-link. In Sections 4 and 5 we analyze how a weak-link affects a ring with *few* or *many* sites respectively. We care to make a bridge between the semiclassical and the “system plus bath” perspectives. Finally we summarize the overall picture in Section 6.

2. Model and Methods

We consider N Bosons in an M site ring that is described by the Bose-Hubbard Hamiltonian (BHH):

$$\mathcal{H}_{\text{BHH}} = \sum_{j=1}^M \left[\frac{U}{2} \mathbf{n}_j (\mathbf{n}_j - 1) - \frac{K_j}{2} \left(e^{i(\Phi/M)} \mathbf{a}_{j+1}^\dagger \mathbf{a}_j + \text{h.c.} \right) \right]. \quad (1)$$

where \mathbf{a}_j (\mathbf{a}_j^\dagger) are bosonic annihilation (creation) operators on the j th site, and $\mathbf{n}_j = \mathbf{a}_j^\dagger \mathbf{a}_j$ is the corresponding number operator. Periodic boundaries are imposed, meaning that $\mathbf{a}_M \equiv \mathbf{a}_0$. The parameter U takes into account the finite scattering length for the atomic two-body collisions on the same site. The hopping parameters are constant $K_j = K$ except in the weak-link where it is K' . The ring is pierced by an artificial (dimensionless) magnetic flux Φ , which can be experimentally induced for neutral atoms as a Coriolis flux by rotating the lattice at constant velocity [19, 20], or as a synthetic gauge flux by imparting a geometric phase directly to the atoms via suitably designed laser fields [21, 22, 23]. The presence of the flux Φ in Eq.(1) has been taken into account through the Peierls substitution: $K_j \rightarrow e^{-i(\Phi/M)} K_j$.

In the quantum analysis, we diagonalize Eq.(1), and display the spectrum as in Fig.1a. For each eigenstate E_ν we calculate the fragmentation measure \mathcal{M} as defined in Appendix B, while the average current is obtained using the following formula:

$$I_\nu = \left\langle E_\nu \left| -\frac{\partial \mathcal{H}}{\partial \Phi} \right| E_\nu \right\rangle \quad (2)$$

In a classical context the average is taken over time for a very long trajectory.

2.1. Semiclassical perspective

For the purpose of semiclassical analysis it is convenient to write the BHH using action-angle variables: $\mathbf{a} \mapsto \sqrt{\mathbf{n}} e^{i\varphi}$. Accordingly the Hamiltonian describes an M degrees of freedom (DOFs) system, namely,

$$H = \sum_{j=1}^M \left[\frac{U}{2} \mathbf{n}_j^2 - K_j \sqrt{\mathbf{n}_{j+1} \mathbf{n}_j} \cos \left(\varphi_{j+1} - \varphi_j - \frac{\Phi}{M} \right) \right] \quad (3)$$

Since the total number of particles $N = \sum \mathbf{n}_j$ is a constant of motion of the system, the Hamiltonian above describes $d = M-1$ coupled pendula. The interaction is characterized by the dimensionless parameter

$$u = \frac{NU}{K} \quad (4)$$

The classical dynamics is governed by

$$\dot{z} = \mathbb{J} \partial H, \quad \mathbb{J} \equiv \begin{pmatrix} 0 & \mathbb{I} \\ -\mathbb{I} & 0 \end{pmatrix} \quad (5)$$

where $z \equiv (\varphi_1, \dots, \varphi_M, \mathbf{n}_1, \dots, \mathbf{n}_M)$ are the canonical coordinates. The notation ∂_μ stands for derivative with respect to z_μ , and \mathbb{J} is the symplectic matrix. It is important

to emphasize that upon re-scaling the only dimensionless parameters that affect the classical trajectories are (u, Φ) and K'/K . The effective Planck constant is $\hbar = 1/N$. The latter parameter, does not appear in the “classical” equations of motion Eq.(5), but only in the full quantum treatment of Eq.(1).

2.2. System plus bath perspective

The conventional approach for analyzing a SQUID/AQUID is based on a “system plus bath” perspective. This perspective becomes meaningful once a weak-link is introduced, which is like having a “slow DOF”. In order to motivate the conventional phenomenology one can regard the BHH Eq.(3) as describing masses that are connected by nonlinear springs. If one spring is very “weak”, then at low energies the equal-partition theorem justifies an harmonic approximation for the small vibrations of the other springs. Accordingly we can regard the system has having one non-linear DOF (“pendulum”) coupled to phonons (“harmonic bath”). The canonical coordinates that describe the weak-link are the phase difference $\varphi = (\varphi_M - \varphi_1)$, and its conjugate $\mathbf{n} = (\mathbf{n}_M - \mathbf{n}_1)/2$. Hence we obtain the Josephson Circuit Hamiltonian (JCH)

$$\mathcal{H}_{\text{JCH}} = E_C \mathbf{n}^2 + \frac{1}{2} E_L \varphi^2 - E_J \cos(\varphi - \Phi) + \mathcal{H}_{\text{bath}} \quad (6)$$

with $E_C = U$, and $E_L = [(N/M)/(M-1)]K$, and $E_J = (N/M)K'$. The bath Hamiltonian has the standard Caldeira-Leggett form

$$\mathcal{H}_{\text{bath}} = \sum_m \left(\frac{1}{2m_m} \tilde{\mathbf{n}}_m^2 + \frac{1}{2} m_m \omega_m^2 \left(\tilde{\varphi}_m - \frac{c_m}{m_m \omega_m^2} \varphi \right)^2 \right) \quad (7)$$

For small M the “bath” is merely a set of several oscillators, and possibly can be neglected, because the ω_m are typically large compared with the natural frequency of the junction. For large M one can characterize the bath oscillators by an Ohmic spectral function

$$J(\omega) \equiv \frac{\pi}{2} \sum_m \frac{c_m^2}{m_m \omega_m} \delta(\omega - \omega_m) = \eta \omega \quad (\omega < \omega_c), \quad (8)$$

The detailed derivation and the explicit expressions for the bath parameters in terms of the BHH parameters are presented in Appendix C, and will be further discussed in a later section. We note that in [12, 5, 14] the finite-temperature partition-function of the BHH ring has been introduced, and the reduced “system plus bath” action has been deduced. From the reduced action one could figure-out what is the effective JCH. In the present approach to the *same* system, we do not assume finite temperature, but merely re-arrange the Hamiltonian in a way that allows a “system plus bath” description. This is a valid procedure even if the ring is prepared (say) in a micro-canonical state with some arbitrary energy E . One may say that in our treatment E/M plays the role of the temperature.

Within the framework of the JCH treatment, the possibility of having metastable

flow-states is controlled by the parameter

$$\alpha \equiv \frac{E_J}{E_L} = (M-1) \frac{K'}{K} \quad (9)$$

For $\Phi = \pi$ the condition for having at least two local minima in the potential floor of the JCH, is $\alpha > \alpha_c$, where $\alpha_c = 1$. Disregarding small quantum fluctuations, the two local minima can support a quasi-degenerate pair of flow-states. If the bath is ignored, then from the WKB approximation it follows that the tunnel splitting is given by some variation of the following expression [12]

$$\Delta_s \approx \sqrt{E_C E_J} \exp \left[-C \sqrt{\frac{E_J}{E_C}} \right] \quad (10)$$

where C is a numerical prefactor. We would like to emphasize that there are several variations of this formula, depending on the relative size of (E_C, E_L, E_J) , but they are all based on the assumption that Eq.(6) is a valid description.

2.3. Two-level system perspective

The objective is obviously to realize a two-level system (TLS) that is quasi-isolated from all the other microscopic DOFs [24, 25, 3, 26, 27, 28, 6]. In the present context there are two flow-states that differ by their “winding number” m , meaning that they are characterized by a different value of the persistent current (I_m). We label these states as \circlearrowleft and \circlearrowright , and write the TLS Hamiltonian as

$$\mathcal{H}_{\text{TLS}} = \begin{pmatrix} E_{\circlearrowleft} & \Delta_s/2 \\ \Delta_s/2 & E_{\circlearrowright} \end{pmatrix} \quad (11)$$

We refer to Δ_s as the splitting: if we draw the eigenenergies versus Φ we get an avoided crossing. The flow-states are required to be meta-stable, meaning that each of them will not decay in time. If they are quasi-degenerate, one would like to witness coherent Rabi oscillations. The quasi-degeneracy is controlled by Φ , and happens for $\Phi = 0$ (say $m = \pm 1$) or for $\Phi = \pi$ (say $m = 0, 1$). During the Rabi oscillation the system evolves into a superposition of these macroscopically distinct flow-states. Such superposition is commonly termed “cat state”.

The conventional procedure to engineer a TLS is as follows: **(i)** To introduce a ring with a weak-link; **(ii)** To ensure that the weak-link DOF is only weakly-coupled to all the other ring DOFs; **(iii)** To analyze the operation of the device using the “system plus bath” paradigm of Caldeira and Leggett. The introduction of a weak-link allows the reduction of the many-body BHH Eq.(1) into the simpler JCH Eq.(6). Furthermore it allows control over the coupling Δ_s between the flow-states. Without a weak-link this coupling might be too small for operational purpose, meaning that the time period ($2\pi/\Delta_s$) of coherent Rabi oscillations might become too large for practical implementations.

If the bath is taken into account then there are two effects. One is “dressing” of the bare parameters, and the other is “noise”. It is well known from the work of Caldeira

and Leggett that coherent Rabi oscillations can be observed provided $\eta < \eta_c$, where η_c is of order unity ($\eta_c = \pi$ for the spin-boson model). We shall come back to this issue when we discuss the large M limit.

3. Coherent dynamics in the absence of a weak-link

The stationary orbitals of a *single* particle in a clean ring are the momentum states with wavenumber $k = (2\pi/M)m$, where m is an integer modulo M . Coherent flow-states have N particles *condensed* into the same momentum orbital:

$$|m\rangle \equiv (\tilde{\mathbf{a}}_m^\dagger)^N |0\rangle \quad (12)$$

Implying a macroscopically large current

$$\mathcal{I}_m = N \times \left(\frac{K}{M}\right) \sin\left(\frac{1}{M}(2\pi m - \Phi)\right) \quad (13)$$

In the absence of interaction ($U = 0$) these coherent flow-states are the eigenstates of the BHH. For $\Phi = \pi$ the $m = 0$ and $m = 1$ flow-states are degenerate in energy. If we add not-too-strong interaction they become coupled and may form a doublet whose dynamics is generated by the TLS Hamiltonian Eq.(11). The energy-difference $\delta E \equiv E_\circ - E_\ominus$ is determined by the deviation $\delta\Phi \equiv (\Phi - \pi)$, and the coupling Δ_s is determined by the strength of the interaction. An example for such doublet is provided in Fig.1.

Assuming that we have a TLS doublet of flow-states with energy splitting Δ_s , one would expect to witness pure Rabi oscillations. If the system has been prepared (say) in a flow-state with clockwise current, the subsequent evolution would be

$$|\Psi(t)\rangle = \cos\left(\frac{\Delta_s t}{2}\right) |\circ\rangle - i \sin\left(\frac{\Delta_s t}{2}\right) |\ominus\rangle \quad (14)$$

implying alternating current with frequency Δ_s , namely,

$$\langle \mathcal{I}(t) \rangle = \cos^2\left(\frac{\Delta_s t}{2}\right) \mathcal{I}_\circ + \sin^2\left(\frac{\Delta_s t}{2}\right) \mathcal{I}_\ominus \quad (15)$$

If we add weak-link or weak-disorder, the flow-states remain stable, provided the perturbation is not too strong. This is the essence of superfluidity. The stability is due to the non-zero interaction U . The interaction stabilizes the flow-states: instead of being located on a flat potential floor, the flow-states are located in local minima of the potential floor. Local minima are structurally-stable with respect to the added disorder, i.e. the local minima do not diminished by a weak perturbation. The common conception is that the two minima are separated by a “forbidden region”. This is the same reasoning that leads to Eq.(10), but here we refer to the multi-dimensional phase-space of the BHH Eq.(3) and not to the reduced single DOF description of Eq.(6). Nevertheless, both perspectives connect smoothly. Namely, we can write Eq.(10) in a way that illuminates the semiclassical expression for tunnel-splitting:

$$\Delta_s \sim \Delta_0 \exp\left[-\frac{C_M}{\hbar} \sqrt{\frac{\alpha}{u}}\right] \quad (16)$$

where $\hbar = 1/N$, while (u, α) are the “classical” parameters, and the prefactor C_M has some dependence on M . In the absence of a weak-link one formally makes the substitution $\alpha \mapsto (M-1)$ as implied by Eq.(9). The energy scale $\Delta_0 \equiv (E_L E_C)^{1/2}$ is like the “attempt frequency” of the Gamow-formula. In a later section we identify Δ_0 as the frequency spacing between the phononic modes.

In the JCH based picture, the splitting Δ_s is exponentially small in N due to the existence of a classically “forbidden region” between the two local minima, which necessitates *tunneling*. This very small Δ_s creates difficulties in witnessing coherent two-level dynamics in such configuration. In order to have a bigger Δ_s a smaller α is required. But it should not be smaller than $\alpha_c = 1$ else the meta-stability is diminished. Note also that there is a trade-off between the weakness of the link and the quality of the superposition state [27].

The question arises whether one can manage without introducing a weak-link. In fact there is a loophole. In order to realize this loophole, one should be aware, following [18], that there are novel flow-states that are not supported by local minima of the potential, but by a “*stability island*” or by a “*chaotic pond*”, or by an “*Arnold web*” region. We summarize all these possibilities in Appendix A - the exact details are not important. The important point is that the phase-space locations, where the flow-states reside, are not separated by a “*forbidden region*”. Instead they are separated by a “*chaotic-sea*”. A visualization of this possibility is provided by the quantum spectrum in Fig.2, which should be contrasted with that of Fig.1. The way we plot the quantum spectrum (following [18]) is in one-to-one correspondence with a section of the classical phase-space: In Fig.1 the two flow-states at the bottom are separated by a “forbidden region” where no states can reside; In contrast to that, in Fig.2, between the two metastable states there are many other states with roughly the same energy that reside in the “chaotic-sea”.

If the coupling between the quasi-degenerate eigenstates is mediated by a chaotic sea, then Δ_s is much larger. This is known as chaos-assisted tunneling [29, 30, 31, 32]. Possibly the term tunneling is not the best description for the mathematics that is involved. The rough idea is that the quantum-coupling between the two metastable states is mediated by some intermediate state in the chaotic sea. The coupling is roughly estimated using second-order perturbation theory as $\Delta_s \sim U^2/\Delta$, where Δ is the detuning from exact resonance. This expression does not contain a WKB suppression exponent, so it is not small, but nevertheless it is very sensitive to the model parameters, as in the theory of universal conductance fluctuations.

In Fig.2 we provide a numerical demonstration of chaos-assisted Rabi oscillations. In this example the device is non-rotating ($\Phi=0$), and the Rabi oscillations are between the metastable $m = \pm 1$ flow-states. The dependence of Δ_s on the number of particles for “chaos assisted tunneling” is contrasted with “under the barrier tunneling” in Fig.3.

Summarizing this section, we observe that the coupling between metastable flow-states can be via chaos-assisted tunneling, implying a relatively large Δ_s when compared with the conventional expectation. A weak-link in a few-site ring is not essential for

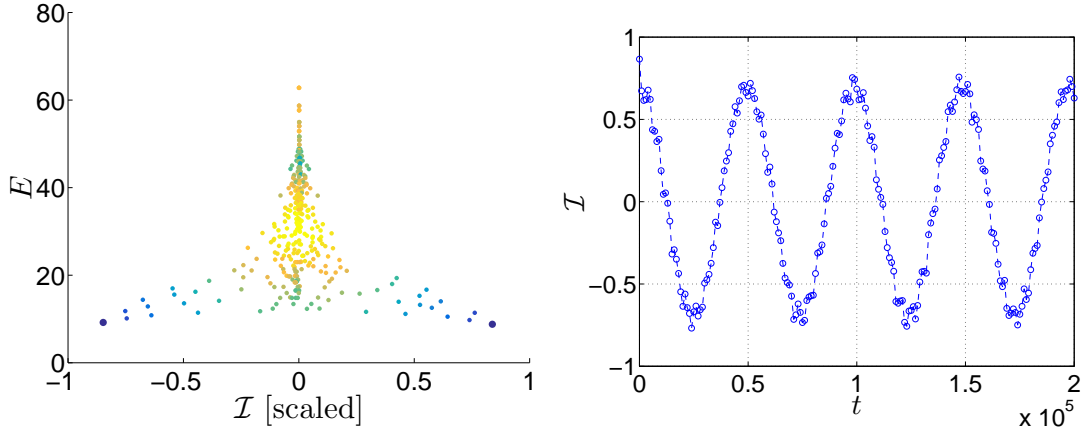


Figure 1. Spectrum of $M=3$ ring with $N=24$ bosons, interaction $u=5$, and $\Phi \sim \pi$ rotation (left panel, a); accompanied with simulation of Rabi oscillations for $\Phi = \pi$ rotation (right panel, b). The units of time (here and in the subsequent figures) are fixed by the hopping frequency $K = 1$. In (a) each point represents an eigenstate, positioned according to its energy E_ν (vertical axis) and its current I_ν (horizontal axis). The current is in units of NK/M . The color encodes the fragmentation of each eigenstate (blue $\mathcal{M} \sim 1$ to red $\mathcal{M} \sim M$). The quasi-degenerate flow-states at the bottom of the energy landscape are energetically-stable (“Landau stability”) and are separated by a forbidden-region. The tunnel-coupling allows coherent Rabi oscillations with extremely slow frequency Δ_s . If we did not slightly perturb Φ , the diagonalization would give zero current cat-states (symmetric and anti-symmetric superposition of the pertinent flow-states). In (b) the initial state is an $m = 1$ coherent state, and the system has exactly $\Phi = \pi$ rotation. This initial state has large overlap with the pair of quasi-degenerate cat eigenstates. Consequently we observe Rabi oscillations of the current with frequency Δ_s that is determined by the tunnel coupling.

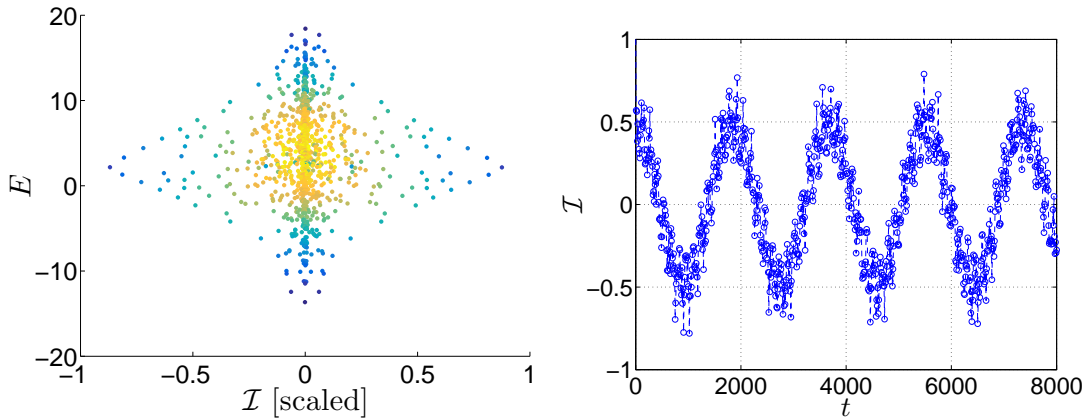


Figure 2. Spectrum of $M=4$ ring with $N=16$ bosons, interaction $u=1$ and $\Phi \sim 0$ rotation (left panel, a); accompanied with simulation of Rabi oscillations (right panel, b). Here the quantum meta-stability of the flow-states $m = \pm 1$ is related to quantum localization on an Arnold web. The coupling is mediated by a chaotic sea. Consequently we observe chaos-assisted coherent Rabi oscillations with relatively short period, which is important for practical qubit implementation.

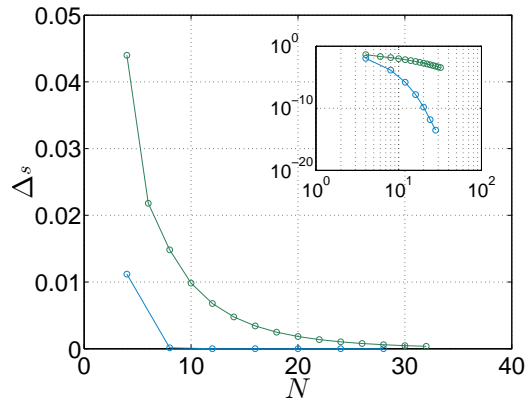


Figure 3. The frequency of the Rabi oscillations Δ_s is plotted as a function of the number of particles N , for an $M = 4$ site ring. The “classical” parameter $u = 1$ is kept constant. The lower curve is the Δ_s for oscillations between $m = 0$ and $m = 1$ at $\Phi = \pi$. The upper curve is the Δ_s for oscillations between $m = +1$ and $m = -1$ for $\Phi = 0$. The large Δ_s in the latter case is due to chaos-assisted tunneling.

getting large Δ_s . In fact its introduction is likely to be harmful for the device operation (see next section).

4. weak-link in a few site ring

In this section we discuss what happens if a weak-link is introduced into a ring that has a small number of sites ($M = 3, 4$). In particular we ask what remains of the JCH phenomenology. The first implication of the JCH phenomenology is the prediction of a critical α below which a quasi-degenerate doublet of flow states cannot exist. If we naively use Eq.(9) we deduce that the condition $\alpha > 1$ for getting such doublet is $K'/K > 1/2$ for $M = 3$ and $K'/K > 1/3$ for $M = 4$. In order to inquire what is the actual threshold we plot quantum spectra for various values of u and K'/K . See Fig.4. We look for doublets at the bottom of the spectrum. A practical measure for that is $\mathcal{M} = [\text{trace}(\rho^2)]^{-1}$, where ρ is the reduced one-body probability matrix, see Appendix B. The value of \mathcal{M} indicates the *fragmentation* of the many-body state. It is $\mathcal{M} = 1$ for a coherent state, and $\mathcal{M} \sim M$ for a quantum-ergodic state. In the case of a doublet the ground-state becomes a superposition of two coherent states hence $\mathcal{M} \sim 2$. Looking at Fig.4 we see that for rings with $M = 3, 4$ sites, the α border is slightly higher than expected. We have verified using Poincare sections (see below) that for large u the border is in agreement with $\alpha_c = 1$. For completeness we also show that for very large u (of order N^2) the value of \mathcal{M} for the ground-state becomes of order M , reflecting the Mott transition [17].

To understand what determines the α_c border we display in Fig.5 so-called Poincare sections of classical trajectories that are generated by the Hamiltonian Eq.(3). Namely, for display purpose a pair of canonical coordinates (Q, P) is selected, and for each trajectory the sequence of points $(Q(t_j), P(t_j))$ where it intersects a specified phase-

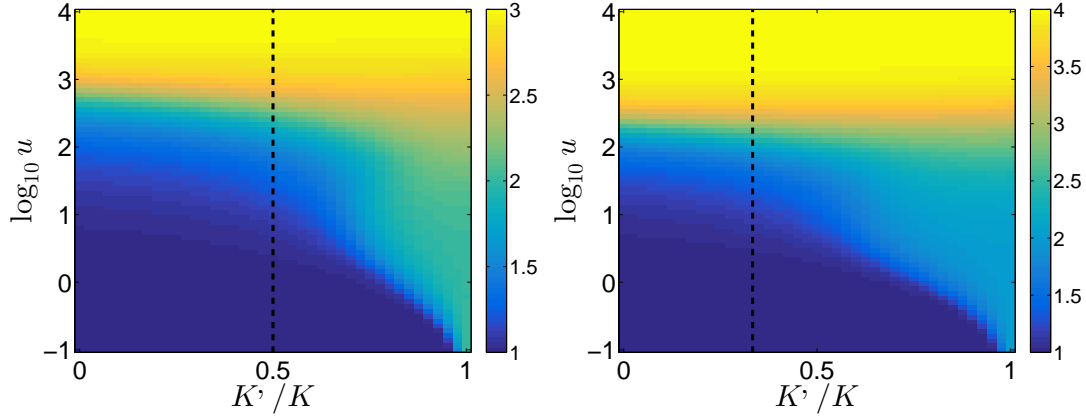


Figure 4. The fragmentation (\mathcal{M}) of the ground state is imaged as a function of u and K'/K for $M=3$ ring with $N=30$ particles (left) and for $M=4$ ring with $N=20$ particles (right). The value $\mathcal{M} = 1$ indicates a coherent state (all particles are condensed in a single orbital). The value of $\mathcal{M} \sim 2$ indicates quasi degeneracy of the ground state (a doublet of flow-states). The value $\mathcal{M} \sim M$ indicates a fragmented state: here it is due to the quantum Mott transition. The vertical dashed line corresponds to the $\alpha_c = 1$ border, which in the absence of a Mott transition would become valid for large u .

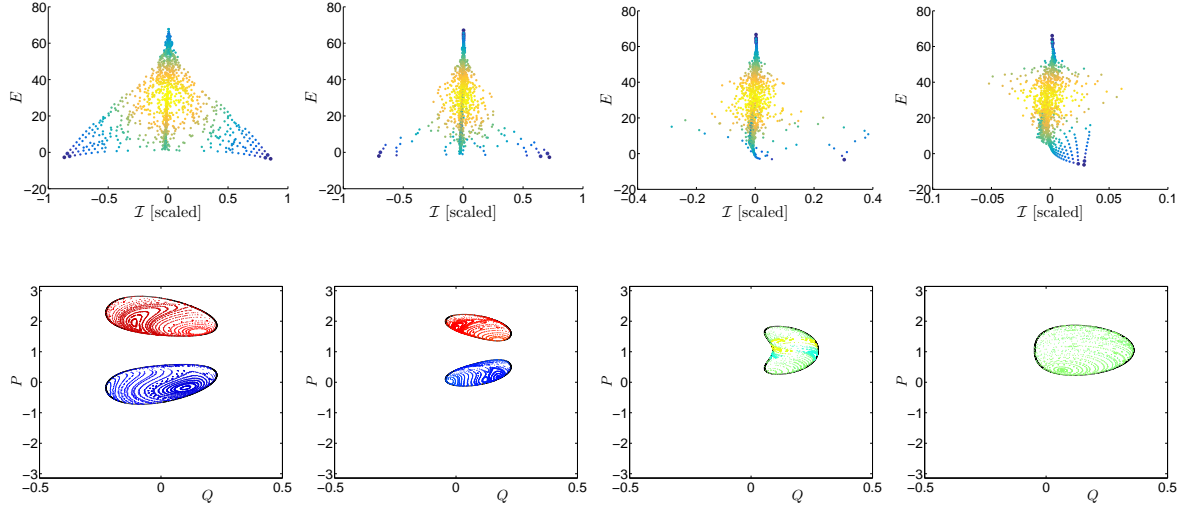


Figure 5. Quantum spectrum (upper panels) and phase-space landscape (lower panels). The quantum spectra are for an $M=3$ ring with $N=45$ particles, dimensionless interaction $u = 2.5$, and weak-link coupling ratio $K'/K = 1, 0.8, 0.65, 0.4$ (from left to right). Axes and color code are the same as in Fig.1. In each case an $n_3 - n_1 = 0$ Poincare section is displayed. The section coordinates are $Q = (n_1 - n_2)/(2N)$ and $P = (\varphi_1 - \varphi_2)$. The energy is chosen to be slightly above the ground state. The solid black line marks the borders of the allowed phase-space regions. The outer regions are “forbidden” energetically. The color code represents the averaged current for each classical trajectory: red for larger clockwise current; blue for large anti-clockwise current; and yellow-to-green for very small current.

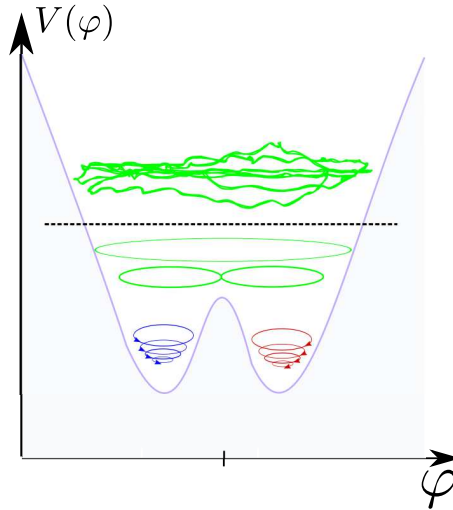


Figure 6. The energy landscape of the Josephson circuit Hamiltonian. Here the vertical axis represents the energy E_φ of the weak-link DOF (the total energy E should include the bath DOFs as well). The dashed line indicates the threshold E_u for chaotic motion. Trajectories below E_u are quasi-regular. The JCH description is valid if E_u is located well above E_b .

space section is recorded. We see clearly that in the $\alpha < \alpha_c$ regime the two stability islands merge, reflecting that we no longer have the “double well” structure in phase space.

But this is not enough. The JCH should be trusted also when we analyze tunneling or phase-slips through the *forbidden region*. For this purpose it should describe correctly the dynamics up to some energy well above the barrier. This means the threshold E_u for chaotic motion should be above the threshold E_b for barrier crossing. See illustration in Fig.6. We therefore plot in Fig.7b, a Poincare section for an energy that is slightly above E_b . What we see is that trajectories that go across the barriers are chaotic rather than regular. This indicates that a JCH description of the dynamics is in fact *not* valid.

Let us try to understand the reason for the failure of the JCH description. In the vicinity of a single flow-state worst case scenario is that a phase difference π has to be supported by the ring. The harmonic approximation requires $\pi/(M-1) < \pi/2$ on each bond. This is marginally satisfied for $M=3$. But if we want the JCH description to be valid over a 2π range of φ , then the requirement becomes $2\pi/(M-1) < \pi/2$, meaning we have to consider rings with $M \geq 5$ sites. Similar claim has appeared in [12]. In Fig.8 we verify that for an $M=6$ ring with weak-link the chaos border E_u is indeed well above the barrier energy E_b . Up to E_u the dynamics looks like that of a pendulum that is slightly affected by the other “bath” DOFs. Above E_u the motion becomes chaotic and the JCH description is no longer applicable.

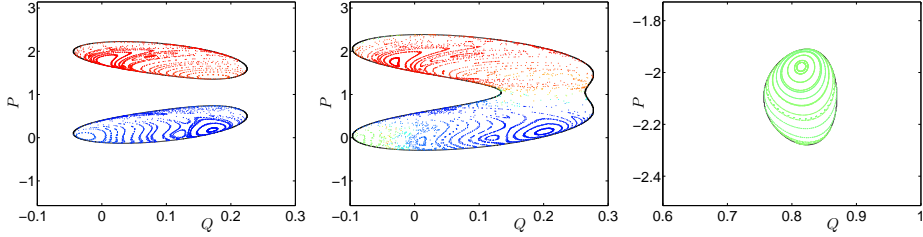


Figure 7. Poincaré sections at different energies. Panel (a) is a zoomed version of Fig.5b. Panels (b) and (c) are for the same model parameters but the total energy is, respectively, $E/N = -0.036$ (slightly above the barrier energy E_b) and $E/N = 1.48$ (close to the upper most energy in the spectrum). In each panel all the trajectories have the same total energy. But if we subtract the bath energy, they correspond to the different trajectories of Fig.6. In panel (c) the island contain self-trapped trajectories, hence it can support self-trapped states (condensation in one site). This should be contrasted with panel (a) where the two islands can support different flow-states (condensation in momentum).

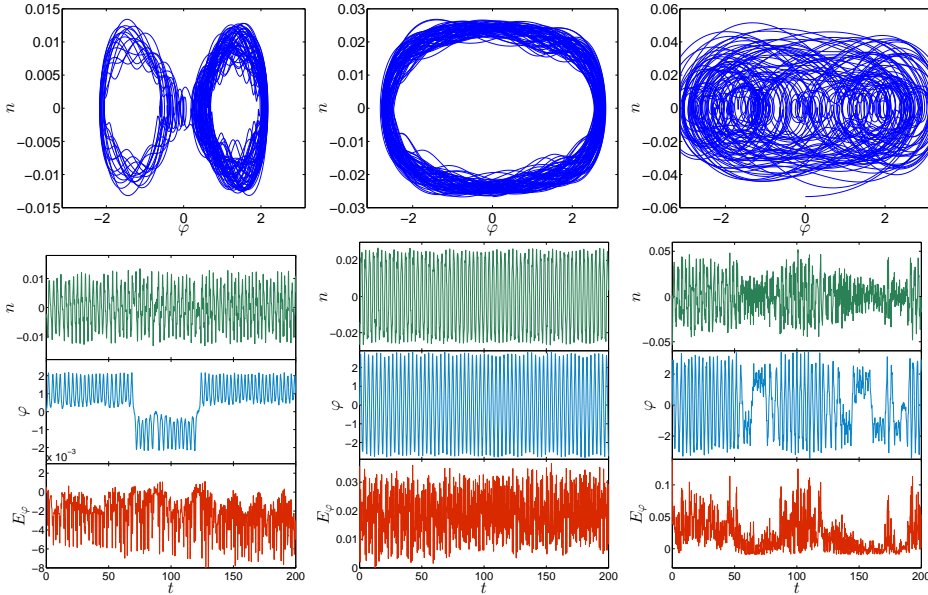


Figure 8. Representative $(\varphi(t), n(t))$ trajectories of an $M=6$ ring with weak-link. The lower panels are for the weak-link energy $E_\varphi(t)$ measured relative to the top of the barrier. The system parameters are $u=200$, and $K_J/K=0.3$, and $\Phi=\pi$. In all the panels the initial condition is in the vicinity of the barrier, with equal populations $n_j = N/6$. The actual starting point is with $n_1 = (1/6 + \delta)N$ and $n_6 = (1/6 - \delta)N$. In (a) the junction energy is mostly below the barrier ($\delta = 0.01$), and we see that the dynamics is in qualitative agreement with the JCH: we observe regular flow-motion with rare jumps to the opposing flow-motion due to an activation by the “bath” DOFs. In (b) the junction energy is above the barrier ($\delta = 0.08$), and we still observe pendulum-like regular motion. In (c) the energy is above the chaos threshold ($\delta = 0.16$), and we get irregular chaotic motion that is no longer described by the JCH. This should be contrasted with the $M = 3$ trajectories of Fig.7b where the chaos threshold E_u coincides with E_b , invalidating the JCH phenomenology.

5. weak-link in a many site ring

Consider N bosons in a ring of length L , such that the average density is $\rho = N/L$. The so called Lieb-Liniger parameter that controls the quantum aspect of the interaction is $\gamma = \mathbf{m}g/\rho$. For $\gamma \gg 1$ the hard-core bosons are like fermions, while for $\gamma \ll 1$ we can use a “classical” description. In the latter case the “trajectories” obey the so-called Gross-Pitaevskii (GP) equation. In fact the parameter γ does not appear in the GP treatment of the model. The only dimensionless parameter of the GP description is

$$u_L = N^2\gamma = NL\mathbf{m}g \quad (17)$$

We shall refer to it as the “classical” dimensionless parameter, while $\hbar = 1/N$ can be regarded as the dimensionless Planck constant. Within the framework of the “classical” (GP) treatment the low excitations of the systems are phonons with sound velocity $c = (g\rho/\mathbf{m})^{1/2}$. For a finite length ring the spacing in the frequencies of the phononic modes is $\Delta_0 = \pi c/L$.

If we add a periodic potential that divides the ring into M sites, we get a system that possibly can be described by the BHH Eq.(1). The analogue of the GP is the discrete nonlinear Schrodinger (DNLS) equation. The distance between the sites is $a = L/M$ and the average number of particles per site is $\bar{n} = N/M$. The effective parameters of the BHH are accordingly $U = g/a$ and

$$K = \frac{1}{\mathbf{m}a^2}e^{-S_0} \equiv \frac{1}{\mathbf{m}^*a^2} \quad (18)$$

where S_0 reflects the height of the barrier. The effective quantum parameter is

$$\gamma^* \equiv \frac{\mathbf{m}^*g}{\rho} = \gamma e^{S_0} = \frac{U}{\bar{n}K} \quad (19)$$

This parameter controls the quantum Mott transition. Namely for $\gamma^* > 1$ superfluidity is diminished if \bar{n} is close to integer. In addition we can define the “classical” dimensionless parameter which is analogous to u_L of Eq.(17) as

$$u_M = Mu = N^2\gamma^* \quad (20)$$

The u_M parameter controls the DNLS equation, and determines the stability of the steady flow solutions, as well as the thresholds for self-trapping and soliton formation. Due to the discretization we have effectively M phononic modes, whose spectrum is characterized by the cutoff frequency

$$\omega_c = (\bar{n}UK)^{1/2} \sim M \Delta_0 \quad (21)$$

Where Δ_0 is formally the same as for a continuous ring, but with m^* .

For a regular ring with a weak-link the reduction to an effective JCH provides the following expressions [4]: $E_C = g/L$ and $E_L = \rho/(\mathbf{m}L)$ and $E_J = \alpha E_L$. The parameter α is controlled by the tunnel-coupling, which is determined by the height of the barrier at the weak-link. Our derivation in Appendix C has provided similar expressions, but there are some differences. First of all the effective mass is of course \mathbf{m}^* and not \mathbf{m} , and therefore the effective quantum parameter γ becomes γ^* . A secondary difference is that

$E_C = g/L$ is replaced by $E_C = g/L^*$, where the effective length over which the density varies might be as small as $L^* = a$. The latter value reflects the extreme case of uniform distribution of the particles along the ring. Expression Eq.(9) for the parameter α can be written as

$$\alpha \equiv \frac{E_J}{E_L} = M e^{-(S_J - S_0)} \quad (22)$$

where S_0 and S_J reflect the heights of the barriers in regular bonds, and at the weak-link respectively.

We turn our attention to the bath. The derivation in Appendix C shows that within the bilinear-coupling approximation the effective number of bath DOFs is $d_{\text{bath}} = \lfloor (M-2)/2 \rfloor$. Consequently the bath Hamiltonian has the familiar Caldeira-Leggett form Eq.(7), with $\mathbf{m}_m = 1/U$, and $\omega_m^2 = 2UK\bar{n}(1 - \cos k_m)$, and $k_m = \pi m/(M-1)$, and $c_m = K\bar{n}[2/(M-1)]^{1/2} \sin k_m$. From that follows that the dissipation coefficient is

$$\eta = \frac{\pi}{\sqrt{\gamma^*}} \quad (23)$$

In Ref.[4], regarding regular ring, it has been claimed that if $(E_J/N) \ll \Delta_0$ (called there “the small ring limit”) then the bath can be ignored. In the context of the present Bose-Hubbard circuit this condition takes the form $K' \ll \omega_c$, meaning that the bath should have high frequency cutoff compared with the hopping rate. But from the work on the spin-boson problem we know that the condition for witnessing coherent oscillation is $\eta < \pi$ which implies that γ^* should be large compared with unity. We identify that this is a problematic non-semiclassical regime where the Mott transition takes place. Namely, for $\gamma^* > 1$ the superfluidity of the system depends sensitively on the filling ratio N/M . In a grand-canonical perspective the system has the tendency to become a Mott insulator.

6. Discussion

We observe that a TLS modeling of quasi-degenerate flow-states in a few-site ring is feasible, meaning that coherent Rabi oscillations are not over-damped. This is true with or without a weak-link, and the frequency is possibly determined by chaos-assistance tunneling. In particular we have demonstrated numerically Rabi oscillations between metastable flow-states in a non-rotating ($\Phi = 0$) circuit that consists of $M = 4$ sites.

We have determined what is the minimal value of α that does not endanger the meta-stability of the $\Phi = \pi$ flow-states. Clearly below this minimal value a weak-link is not useful. From a semi-classical perspective this value is the threshold for the merging of two stability islands. For large rings, assuming that the JCH phenomenology is valid, the minimal value is implied by the familiar condition $\alpha > \alpha_c$ with $\alpha_c = 1$. We note that in a superconducting circuit, due to the Meisner effect, the effective inductance is larger, and α is typically large.

In the semiclassical perspective the flow-states are supported by a local minimum of the energy landscape (Landau stability), or by a region that is surrounded by KAM tori. In the latter case, for rings with $M > 3$ sites the stabilization is due to a many-body quantum localization effect, that suppresses the Arnold diffusion. Depending on the type of states involved, the coupling might be via a forbidden-region (as implied by the JCH phenomenology), or it might be mediated by a chaotic sea. In the latter case the chaos-assisted tunneling provides a weaker dependence on the number of particles involved.

The system plus bath perspective.— Formally the circuit has $d = M - 1$ interacting DOFs, while in the approximated JCH version we have a single DOF (φ, \mathbf{n}) that interacts with a “bath” that consists of a few DOFs. If the bath is ignored the motion in the single DOF phase-space is regular, and looks formally the same as that of a pendulum. If $\alpha > \alpha_c$, a separatrix is formed, hence we have two stability-islands that can support the two quasi-degenerate flow-states. But if the bath is taken into account, the projected motion in the (φ, \mathbf{n}) coordinates becomes “dressed” and “noisy”, in the same sense as discussed by Caldeira, Leggett and followers. These effects endanger the coherent Rabi oscillations.

Large M ring.— Considering a regular ring with bosons one can define the Lieb-Liniger parameter γ . For $\gamma > 1$ the quantum effects become important (GP description becomes problematic), but nevertheless there is no quantum phase-transition from superfluid to insulator. Considering the BHH ring (Bose gas in an optical lattice), we have defined an effective γ^* that corresponds to the effective mass in the lattice. For $\gamma^* > 1$ the quantum effects are dramatic, namely, a transition to the Mott-regime, where depending on the filling-ratio the ring can become a Mott-insulator. But the analysis shows that $\gamma^* > 1$ is the condition for witnessing coherent Rabi oscillations. So there is a clash here: on the one hand we want the ring to be in a superfluid phase (avoid Mott); on the other hand we want to have weak coupling to the bath in order to witness coherent oscillations.

Small M ring.— We wanted to understand how this standard JCH phenomenology is modified if the ring consists of a small number of sites. Then the “bath” consists of a small number of DOFs and the standard Caldeira-Leggett perspective becomes questionable. One direction [33] is to say that the interaction with *chaotic* DOFs is essentially like the interaction with infinitely many *harmonic* DOFs, hence coming back to Caldeira-Leggett phenomenology. This type of argument might work for rings with $M \geq 6$ sites for which the effective number of bath DOFs is $d_{\text{bath}} \geq 2$. We did not take this route here. Rather we discussed the whole issue in a much more fundamental level, focusing on rings with small number of sites.

Interaction with a chaotic surrounding is the low dimensional version of having a “bath”. Even for weak chaos there is so-called Arnold-diffusion that is induced by the stochastic motion (“noise”) of the other DOFs. It follows rigorously that a necessary condition for the applicability of the “system plus bath” paradigm with regard to a circuit with a weak-link requires more than 3 sites. But this is not a sufficient condition. We have emphasized that a JCH modeling implies regular motion up to an energy that exceeds the barrier height. Such high threshold for chaos is apparently feasible only for rings that have more than 5 sites.

Acknowledgements.— We thank Luigi Amico for motivating the present study. This research has been supported by the Israel Science Foundation (grant No. 29/11).

Appendix A. Superfluidity in low dimensional circuits

In this Appendix we provide a brief summary for the “big picture” of mesoscopic superfluidity. The key issue is the meta-stability of the flow-states. We follow [18], while some preliminaries regarding the energy landscape and the dynamical stability issues can be found in [17] and [34] respectively.

In the conventional “Landau criterion” picture the flow-states are energetically stable, i.e. they are located in local minima of the energy landscape. Hence they are separated by a “forbidden region” and the coupling requires tunneling.

But metastability can be achieved even in the absence of energetic-stability. For $M = 3$ ring, the flow-state can be dynamically stable, protected in phase-space by Kolmogorov Arnold and Moser (KAM) tori. Then the generic picture is two islands that are separated by a chaotic sea, and not by a forbidden region.

For $M > 3$ rings, the KAM tori are not able to divided phase-space into territories. The dynamics takes place on an “Arnold web” of resonances. This leads to so-called Arnold diffusion: if we look on the weak-link degree of freedom (φ, n) we expect to see diffusion of its energy. We emphasize that such diffusion does not occur in $M = 3$ ring: there it is arrested by the KAM tori.

The discussion above might give the impression that flow-states cannot survive in $M > 3$ rings. But in fact quantum mechanics saves us: dynamical stability can be maintained in-spite of Arnold diffusion. This can be regarded as a many-body localization effect. It follows from the following simple consideration: The time to escape an Arnold web region might be very long; if the required time is larger than the quantum brektime (inverse level spacing) then the escape will never happen.

Appendix B. Definition of the fragmentation measure \mathcal{M}

The eigenstates of the Hamiltonian Eq.(1) can be characterized by their fragmentation $\mathcal{M} = [\text{trace}(\rho^2)]^{-1}$, where the one-body reduced probability matrix is

$$\rho_{ij} = \frac{1}{N} \langle \mathbf{a}_j^\dagger \mathbf{a}_i \rangle \quad (\text{B.1})$$

Roughly speaking \mathcal{M} tells us how many orbitals are occupied by the bosons. A value of $\mathcal{M} = 1$ indicates that the state it not fragmented, hence it can be written as $(b_k^\dagger)^N |\text{vacuum}\rangle$. Here $b_k^\dagger = \sum_j c_j^k a_j^\dagger$ creates a particle in some superposition of the site modes, with coefficients c_j^k . Such states are the many-body coherent-states in the generalized sense of Perelomov [35]. Their phase-space representations are minimal wave packets situated at some point (φ, \mathbf{n}) of phase space. A higher value $1 < \mathcal{M} \leq M$ indicates that the bosons are fragmented into several orbitals.

Appendix C. Derivation of the Josephson Circuit Hamiltonian

Consider N Bosons in an M site ring described by the BHH Eq.(1). In the limit $u \gg M$ it is common to neglect the fluctuations of the number of atoms in each well [36], and approximate the Bose-Hubbard model with the so called quantum-phase-model (“coupled rotors”) which is formally equivalent to an array of Josephson junctions:

$$\mathcal{H} = \sum_{j=1}^M \left[\frac{U}{2} \mathbf{n}_j^2 - \bar{n} K_j \cos \left((\varphi_{j+1} - \varphi_j) - \frac{\Phi}{M} \right) \right] \quad (\text{C.1})$$

Where \mathbf{n}_j and φ_j are canonically conjugate variables. Without lost of generality, we can employ a gauge transformation such that the phase Φ vanishes at all bonds except the weak-link. Namely,

$$\mathcal{H} = \sum_{j=1}^M \frac{U}{2} \mathbf{n}_j^2 - \bar{n} K \sum_{j=1}^{M-1} \cos(\varphi_{j+1} - \varphi_j) - \bar{n} K' \cos(\varphi_1 - \varphi_M - \Phi) \quad (\text{C.2})$$

With a weak-link $K' \ll K$, the phase difference at the $M - 1$ regular bonds becomes small such that $\cos(\varphi_{j+1} - \varphi_j) \sim 1$. The Hamiltonian can then be written, up to a constant, as:

$$\mathcal{H} = \sum_{j=1}^M \frac{U}{2} \mathbf{n}_j^2 + \frac{\bar{n} K}{2} \sum_{j=1}^{M-1} (\varphi_{j+1} - \varphi_j)^2 - \bar{n} K' \cos(\varphi_1 - \varphi_M - \Phi) \quad (\text{C.3})$$

The second sum can be written as:

$$\sum_{j=1}^{M-1} (\varphi_{j+1} - \varphi_j)^2 = \varphi_1^2 + \varphi_M^2 - 2\varphi_1\varphi_2 - 2\varphi_{M-1}\varphi_M + \sum_{i,j=2}^{M-1} A_{ij} \varphi_i \varphi_j \quad (\text{C.4})$$

$$= \frac{\varphi_+^2}{2} + \frac{\varphi_-^2}{2} - \varphi_+(\varphi_2 + \varphi_{M-1}) - \varphi_-(\varphi_2 - \varphi_{M-1}) + \sum_{i,j=2}^{M-1} A_{ij} \varphi_i \varphi_j \quad (\text{C.5})$$

Where we introduced the notation $\varphi_{\pm} = \varphi_1 \pm \varphi_M$, and $A_{ij} = 2\delta_{ij} - \delta_{i,j\pm 1}$. Consequently

$$\begin{aligned} \mathcal{H} &= \frac{U}{4} (\mathbf{n}_-^2 + \mathbf{n}_+^2) + \frac{\bar{n} K}{4} (\varphi_-^2 + \varphi_+^2) \\ &\quad - \bar{n} K' \cos(\varphi_- - \Phi) - \frac{\bar{n} K}{2} [\varphi_-(\varphi_2 - \varphi_{M-1}) + \varphi_+(\varphi_2 + \varphi_{M-1})] \\ &\quad + \frac{U}{2} \sum_{j=2}^{M-1} \mathbf{n}_j^2 + \frac{\bar{n} K}{2} \sum_{i,j=2}^{M-1} A_{ij} \varphi_i \varphi_j \end{aligned} \quad (\text{C.6})$$

The last line can be easily diagonalized:

$$\frac{U}{2} \sum_{j=2}^{M-1} \mathbf{n}_j^2 + \frac{\bar{n} K}{2} \sum_{i,j=2}^{M-1} A_{ij} \varphi_i \varphi_j = \sum_{m=1}^{M-2} \left(\frac{U}{2} \tilde{\mathbf{n}}_m^2 + \frac{\omega_m^2}{2U} \tilde{\varphi}_m^2 \right) \quad (\text{C.7})$$

with

$$\omega_m^2 = 2UK\bar{n}(1 - \cos k_m) \quad (\text{C.8})$$

$$k_m = \pi m / (M - 1) \quad (\text{C.9})$$

$$\tilde{\varphi}_m = \sqrt{\frac{2}{M-1}} \times \sum_{j=2}^{M-1} \sin[k_m(j-1)] \varphi_j \quad (\text{C.10})$$

Due to the reflection symmetry of the “chain” ($j = 2, \dots, M - 1$), the $m = \text{odd}$ and $m = \text{even}$ modes are symmetric and anti-symmetric respectively. The coupling term $\varphi_{\pm}(\varphi_2 \pm \varphi_{M-1})$ can be expressed as follows:

$$\varphi_{\pm} \sqrt{\frac{2}{M-1}} \times \sum_{m=1}^{M-2} [\sin(k_m) \pm \sin(k_m(M-2))] \tilde{\varphi}_m \quad (\text{C.11})$$

$$= \varphi_{\pm} \sqrt{\frac{2}{M-1}} \times \sum_{m=1}^{M-2} \sin(k_m) [1 \pm (-1)^{m-1}] \tilde{\varphi}_m \quad (\text{C.12})$$

We see that φ_+ is coupled only to the symmetric modes ($m = \text{odd}$), while φ_- is coupled only to the anti-symmetric modes ($m = \text{even}$). With the above substitutions the Hamiltonian takes the form:

$$\mathcal{H} = \frac{U}{4} (\mathbf{n}_-^2 + \mathbf{n}_+^2) + \frac{\bar{n}K}{4} (\varphi_-^2 + \varphi_+^2) - \bar{n}K' \cos(\varphi_- - \Phi) \quad (\text{C.13})$$

$$- \varphi_- \sum_{m=\text{even}}^{M-2} c_m \tilde{\varphi}_m - \varphi_+ \sum_{m=\text{odd}}^{M-2} c_m \tilde{\varphi}_m + \sum_{m=1}^{M-2} \left(\frac{U}{2} \tilde{\mathbf{n}}_m^2 + \frac{\omega_m^2}{2U} \tilde{\varphi}_m^2 \right) \quad (\text{C.14})$$

with

$$c_m = K\bar{n}[2/(M-1)]^{1/2} \sin k_m \quad (\text{C.15})$$

The Hamiltonian consist of the two freedoms ψ_{\pm} which are coupled to an harmonic bath of $M-2$ DOFs. But in-fact only the weak-link DOF ψ_- and the $m = \text{even}$ modes of the bath are of interest. The freedom ψ_+ can be thought of as a part of the $m = \text{odd}$ modes of the bath, which does not interact with the weak-link. So that the relevant part of the Hamiltonian is:

$$\mathcal{H} = U\mathbf{n}^2 + \frac{\bar{n}K}{4} \varphi^2 - \bar{n}K' \cos(\varphi - \Phi) \quad (\text{C.16})$$

$$- \varphi \sum_{m=\text{even}}^{M-2} c_m \tilde{\varphi}_m + \sum_{m=\text{even}}^{M-2} \left(\frac{U}{2} \tilde{\mathbf{n}}_m^2 + \frac{\omega_m^2}{2U} \tilde{\varphi}_m^2 \right) \quad (\text{C.17})$$

where we have changed the notations, namely $\varphi = \varphi_-$ and the conjugate $\mathbf{n} = \mathbf{n}_-/2$. The effective number of bath DOFs is

$$d_{\text{bath}} = \lfloor (M-2)/2 \rfloor \quad (\text{C.18})$$

Re-writing the bath in the standard Caldeira-Leggett form Eq.(7) the JCH takes the form

$$\mathcal{H} = U\mathbf{n}^2 + \frac{\bar{n}K}{4} \varphi^2 - \bar{n}K' \cos(\varphi - \Phi) + V_{\text{counter}} + \mathcal{H}_{\text{bath}} \quad (\text{C.19})$$

In order to get Eq.(6) one has to do some algebra with the counter-term:

$$V_{\text{counter}} = -\varphi^2 \sum_{m=\text{even}}^{M-2} \frac{U c_m^2}{2\omega_m^2} = -\varphi^2 \frac{\bar{n}K}{2(M-1)} \sum_{m=\text{even}}^{M-2} \frac{\sin^2 k_m}{1 - \cos k_m} \quad (\text{C.20})$$

$$= -\varphi^2 \frac{\bar{n}K}{M-1} \sum_{m=\text{even}}^{M-2} \cos^2 \left(\frac{k_m}{2} \right) = -\frac{1}{4} \left(\frac{M-3}{M-1} \right) \bar{n}K \varphi^2 \quad (\text{C.21})$$

References.—

- [1] Seaman B, Krämer M, Anderson D and Holland M 2007 *Phys. Rev. A* **75** 023615
- [2] Pepino R, Cooper J, Anderson D and Holland M 2009 *Phys. Rev. Lett.* **103** 140405
- [3] Hallwood D W, Burnett K and Dunningham J 2006 *New J. Phys.* **8** 180–180
- [4] Solenov D and Mozyrsky D 2010 *Phys. Rev. Lett.* **104**(15) 150405 [link]
- [5] Amico L, Aghamalyan D, Auksztol F, Crepaz H, Dumke R and Kwek L C 2014 *Sci. Rep.* **4** [link]
- [6] Aghamalyan D, Cominotti M, Rizzi M, Rossini D, Hekking F, Minguzzi A, Kwek L C and Amico L 2015 *New J. Phys.* **17** 045023
- [7] Amico L, Osterloh A and Cataliotti F 2005 *Phys. Rev. Lett.* **95**(6) 063201 [link]
- [8] Wright K C, Blakestad R B, Lobb C J, Phillips W D and Campbell G K 2013 *Phys. Rev. Lett.* **110**(2) 025302 [link]
- [9] Eckel S, Lee J G, Jendrzejewski F, Murray N, Clark C W, Lobb C J, Phillips W D, Edwards M and Campbell G K 2014 *Nature* **506** 200–203 [link]
- [10] Cominotti M, Rossini D, Rizzi M, Hekking F and Minguzzi A 2014 *Phys. Rev. Lett.* **113**(2) 025301 [link]
- [11] Ryu C, Blackburn P W, Blinova A A and Boshier M G 2013 *Phys. Rev. Lett.* **111**(20) 205301 [link]
- [12] Rastelli G, Pop I M and Hekking F W J 2013 *Phys. Rev. B* **87**(17) 174513 [link]
- [13] Manucharyan V E, Koch J, Glazman L I and Devoret M H 2009 *Science* **326** 113–116 [link]
- [14] Rastelli G, Vanevic M and Belzig W 2015 *New J. Phys.* **17** 053016
- [15] Koch J, Manucharyan V, Devoret M and Glazman L 2009 *Phys. Rev. Lett.* **103** 217004
- [16] Leggett A J 1980 *Prog. Theor. Phys. Suppl.* **69** 80–100
- [17] Arwas G, Vardi A and Cohen D 2014 *Phys. Rev. A* **89**(1) 013601 [link]
- [18] Arwas G, Vardi A and Cohen D 2015 *Sci. Rep.* **5** 13433 [link]
- [19] Fetter A L 2009 *Rev. Mod. Phys.* **81** 647
- [20] Wright K, Blakestad R, Lobb C, Phillips W and Campbell G 2013 *Phys. Rev. Lett.* **110** 025302
- [21] Leanhardt A, Görlitz A, Chikkatur A, Kielpinski D, Shin Y, Pritchard D and Ketterle W 2002 *Phys. Rev. Lett.* **89** 190403
- [22] Lin Y J, Compton R L, Jimenez-Garcia K, Porto J and Spielman I B 2009 *Nature* **462** 628–632
- [23] Dalibard J, Gerbier F, Juzeliūnas G and Öhberg P 2011 *Rev. Mod. Phys.* **83** 1523
- [24] Rey A M, Burnett K, Satija I I and Clark C W 2007 *Phys. Rev. A* **75** 063616
- [25] Nunnenkamp A, Rey A M and Burnett K 2008 *Phys. Rev. A* **77** 023622
- [26] Hallwood D W, Stokes A, Cooper J J and Dunningham J 2009 *New J. Phys.* **11** 103040
- [27] Nunnenkamp A, Rey A M and Burnett K 2011 *Phys. Rev. A* **84** 053604
- [28] Nunnenkamp A, Rey A M and Burnett K 2010 *Proc. R. Soc. A* **466** 1247–1263
- [29] Tomsovic S and Ullmo D 1994 *Phys. Rev. E* **50**(1) 145–162 [link]
- [30] Steck D A 2001 *Science* **293** 274–278 [link]
- [31] Hensinger W K, Häffner H, Browaeys A, Heckenberg N R, Helmerson K, McKenzie C, Milburn G J, Phillips W D, Rolston S L, Rubinsztein-Dunlop H *et al.* 2001 *Nature* **412** 52–55
- [32] Averbukh V, Osovski S and Moiseyev N 2002 *Phys. Rev. Lett.* **89**(25) 253201 [link]
- [33] Cohen D and Kottos T 2004 *Phys. Rev. E* **69**(5) 055201 [link]
- [34] Wu B and Niu Q 2003 *New J. Phys.* **5** 104 [link]
- [35] Perelomov A 1972 *Communications in Mathematical Physics* **26** 222–236 ISSN 0010-3616 [link]
- [36] Paraoanu G S 2003 *Phys. Rev. A* **67**(2) 023607 [link]